$1+1$ is Greater Than 2: Collaborative Automotive Radar Imaging Exploiting Spatial Diversity

Shunqiao Sun[†], Changzhi Li[‡]

[†]Department of Electrical and Computer Engineering, The University of Alabama, USA

[‡]Department of Electrical and Computer Engineering, Texas Tech University, USA

***Abstract*— Automotive radar provides superior performance for autonomous vehicles over camera and LiDAR in harsh environment. However, the performance of single automotive radar is subject to either small aperture or limited field of view. It is of great interests to improve the automotive radar imaging performance with an automotive radar network. In this paper, we propose a distributed iterative adaptive approach based collaborative automotive radar imaging using an automotive radar network consisting of heterogeneous automotive radars. Under the proposal, raw radar measurement is not shared. Instead, by exploiting the spatial diversity, each automotive radar fuses the intermediate local imaging estimations with adjacent neighboring radars. Numerical results demonstrate the performance improvement of the collaborative radar imaging.**

***Keywords*— automotive radar network, collaborative radar imaging, autonomous driving.**

I. Introduction

Millimeter-wave automotive radar has strong penetration capabilities in fog, rain, snow, smoke, and dust, making it robust to inclement weather conditions [1]–[4]. The fully autonomous vehicles would require dense point clouds or radar imaging with high angular resolution close to LiDAR [3], [5] to support object detection and classification. It is of great interests to develop automotive radar network consisting of multiple automotive radars with small form factors and low-cost to jointly sensing the surrounding environment.

Automotive radar network [6]–[11] offers numerous benefits for object detection and radar imaging over single automotive radar sensor. Such radar networks may operate in coherent [9] or non-coherent ways [8]. By coherently combining the measurement from every subarray, it is shown in [9] that direction-of-arrival (DOA) estimation with a high-resolution corresponding to a whole array with large aperture can be achieved. The coherent process requires to know the exact subarray locations which is challenging for radars on moving platforms. For distributed antenna arrays, the isotropic scattering model does not hold. It is shown in [10] that a non-coherent radar network connected via wire in a single vehicle can improve the detection performance over a single radar module by exploiting spatial diversity. The radar networks achieve these performance improvements at a cost of high operating complexity. Usually, all the sensors in the network need to be synchronized, either via wire for radar sensors deployed in the same vehicle [7], [10] or via wireless for radar sensors deployed on different vehicles [12]. Clock synchronization with open-loop and close-loop schemes was investigated in [13] for distributed beamforming. A wireless communication link, such as vehicle-to-everything (V2X) [14], is required to share the sensors measurements or estimation results in radar network.

In this paper, we propose a distributed collaborative radar imaging approach to iteratively fuse the radar imaging from distribute automotive radars exploiting frequency-modulated continuous-wave (FMCW) in a non-coherent way without sharing the raw radar measurements. The approach can be extended to other waveforms, such as phased-modulated continuous-wave (PMCW), which allows to achieve joint radar-communication functions [15]. However, we assume massive raw measurement data at radar sensors are not shared via the wireless communication link. As a result, the bistatic operation of the radar network is not considered. The radar measurements are remained at the edge devices. Under the proposed framework, the radar network is operating in an ad hoc mode, and there is no requirement of a central control unit or server to collect all the sharing data from all radar devices. Instead, each automotive radar shares its intermediate estimation results with its neighbors.

II. System Model

On urban streets, vehicles may join or leave a radar network in a random fashion. Fig. 1 shows an example of collaborative radar imaging of a cross street area of interest with two automotive radars deployed on adjacent vehicles.

Each automotive radar transmits FMCW waveforms, with the transmit frequency, $f_T(t)$, changing linearly with time, i.e., $f_T\left(t\right) = f_c + \frac{B}{T}t$, where f_c, B, and T are carry frequency, bandwidth and chirp duration, respectively. The phase $\varphi_T(t)$ of the transmitted signal could be obtained after integration as $\varphi_T\left(t\right) = 2\pi\int_{-T/2}^{t} f_T\left(t\right)dt$. The noiseless received signal is a delayed version of the transmitted signal. For a target at a range of R with a radial velocity of v, the round-trip delay can be expressed as $\tau = 2(R+vt)/c$, where c is the speed of light. The received signal is mixed with the transmit signal, and the output of the mixer is the beat signal, whose phase could be approximated as [1]

$$\varphi_B(t) = 2\pi\left[\frac{2f_cR}{c} + \left(\frac{2f_cv}{c} + \frac{2BR}{Tc}\right)t\right], \qquad (1)$$

where the beat frequency is $f_b = f_R + f_D$ with $f_R = \frac{2BR}{Tc}$ and $f_D = \frac{2f_cv}{c}$ being the range and Doppler frequency.

Assume there are K targets in far-field with range R_k, velocity v_k, azimuth angle θ_k and radar cross section (RCS) β_k, for $k = 1, \cdots, K$. Consider a receive antenna array with N elements. After de-chirping, the received signal of the antenna array is

$$\mathbf{y}(t) = [y_1(t), y_2(t), \cdots, y_N(t)]^T, \tag{2}$$

with

$$y_n(t) = \sum_{k=1}^{K} \beta_k e^{j2\pi\left[\left(f_D^k + f_R^k\right)t + \frac{d_n \sin(\theta_k)}{\lambda}\right]} + e_n(t), \tag{3}$$

where $f_D^k = \frac{2f_c v_k}{c}$, $f_R^k = \frac{2BR_k}{Tc}$. Here, d_n is the distance of the n-th antenna array element to the reference element; $\lambda = c/f_c$ is the wavelength, and $e_n(t)$ is the additive noise.

At each receive antenna, the receive signal is sampled with a sampling frequency of $f_s \geq f_b^{\max}$, where $f_b^{\max}$ is the maximum beat frequency that is determined by the maximum unambiguous detectable range $R_{\max}$, as the $f_D^{\max} \ll f_R^{\max}$ in automotive radars [1]. The number of samples in fast-time is $N_F = \lfloor T/T_s \rfloor$, where $T_s = 1/f_s$ is the sampling interval. The sampled data collected from N receive antennas can be written as

$$\mathbf{Y} = [\mathbf{y}(1), \mathbf{y}(2), \cdots, \mathbf{y}(N_F)] \in \mathbb{C}^{N \times N_F}, \tag{4}$$

where $\mathbf{y}(n') = \mathbf{y}((n'-1)T_s)$ for $n' = 1, \cdots, N_F$. The samples can be rearranged as $\mathbf{d} = \text{vec}(\mathbf{Y}) \in \mathbb{C}^{NN_F \times 1}$. Discrete the maximum unambiguous detectable range and azimuth angle field of view (FOV) with fine grid size of Δr and $\Delta\theta$, respectively. Let P and Q respectively denote the number of discrete ranges and angles. Since the change of Doppler frequency in fast-time is negligible [1], we define a dictionary matrix $\mathbf{B}$ containing only the delays and angles information in below.

$$\mathbf{B} = [\mathbf{b}_{1,1}, \cdots, \mathbf{b}_{1,Q}, \mathbf{b}_{2,1}, \cdots, \mathbf{b}_{P,Q}] \in \mathbb{C}^{NN_F \times PQ}, \tag{5}$$

where $\mathbf{b}_{p,k} = \left[\mathbf{x}_{p,k}^T(1), \cdots, \mathbf{x}_{p,k}^T(N_F)\right]^T$ with

$$\mathbf{x}_{p,k}(n') = e^{j2\pi f_R^p (n'-1)T_s} \mathbf{a}(\theta_k), n' = 1, \cdots, N_F \tag{6}$$

and

$$\mathbf{a}(\theta_k) = \left[e^{j\frac{2\pi d_1 \sin(\theta_k)}{\lambda}}, \cdots, e^{j\frac{2\pi d_N \sin(\theta_k)}{\lambda}}\right]^T \in \mathbb{C}^{N \times 1}. \tag{7}$$

Therefore, the receive samples can be represented as

$$\mathbf{d} = \mathbf{B}\boldsymbol{\beta} + \mathbf{e}, \tag{8}$$

where

$$\boldsymbol{\beta} = [\beta_{1,1}, \cdots, \beta_{1,Q}, \beta_{2,1}, \cdots, \beta_{P,Q}]^T \in \mathbb{C}^{PQ \times 1}, \tag{9}$$

and $\mathbf{e} \in \mathbb{C}^{NN_F \times 1}$ is the noise term. The radar imaging task is to estimate the target reflection coefficients $\boldsymbol{\beta}$ from the measurement data $\mathbf{d}$. The model is easy to extend to automotive MIMO radar by utilizing multiple transmit antennas and multiple receive antennas.

A. *Collaborative Automotive Radar Imaging*

We consider collaborative radar imaging of the common area of interests with L automotive radars on different automobiles. Each automotive radar may have different antenna array geometry with different aperture size and different number of antenna elements. The measurement data of the automotive radar on the l-th automobile is

$$\mathbf{d}_l = \mathbf{B}_l \boldsymbol{\beta}_l + \mathbf{e}_l, \tag{10}$$

where $\mathbf{B}_l \in \mathbb{C}^{N_l N_F \times PQ}$ is the dictionary matrix of the l-th radar with N_l receive antennas, and $\boldsymbol{\beta}_l$ is the target RCS vector. In general, the target RCS vectors measured by different radars are different, i.e., $\boldsymbol{\beta}_i \neq \boldsymbol{\beta}_j$ for $i \neq j$, because the range and angle estimations of the same targets on different radars at different automobiles are in general different. In addition, due to spatial diversity, the RCS magnitudes of the same targets are hardly measured identically by radars on different automobiles. In this paper, we adopt a constraint such that the estimated global image is an average of the local images [16]. Different from [16], sparsity imaging assumption is not required in our model.

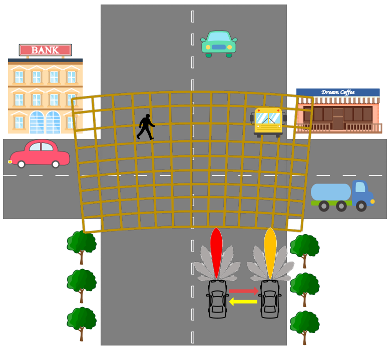

Fig. 1. Example of collaborative radar imaging with multiple radars deployed on adjacent vehicles. Automotive radars share their estimation results via the V2X technology.

The collaborative imaging problem using all the L automotive radars measurements can be formulated as

$$\begin{aligned} \min \quad & \sum_{l=1}^{L} \|\mathbf{d}_l - \beta_{l,p,k}\mathbf{b}_{l,p,k}\|_{\mathbf{Q}_{l,p,k}^{-1}}^2 \\ \text{s.t.} \quad & \frac{1}{L}\sum_{l=1}^{L} \mathbf{T}_l \boldsymbol{\beta}_l = \boldsymbol{\beta}_G, \quad l = 1, \cdots, L. \end{aligned} \tag{11}$$

Here, $\mathbf{Q}_{l,p,k}$ is the interference covariance matrix on the l-th radar, and $\boldsymbol{\beta}_G = [\beta_{1,1}, \cdots, \beta_{1,Q}, \beta_{2,1}, \cdots, \beta_{P,Q}]^T$ is the RCS vector under the global coordinate, and $\mathbf{T}_l \in \mathbb{C}^{PQ \times PQ}$ is a shifting matrix to transform the RCS vector estimated from the radar on the l-th automobile to the global coordinate. The collaborative imaging problem (11) can be solved via the alternative direction method of multipliers (ADMM) [17]. The augmented Lagrangian is

$$\begin{aligned} f_{p,k} = & \frac{1}{2}\sum_{l=1}^{L} \|\mathbf{d}_l - \beta_{l,p,k}\mathbf{b}_{l,p,k}\|_{\mathbf{Q}_{l,p,k}^{-1}}^2 + \sigma_{p,k}\left(\bar{\beta}_{p,k} - \beta_{p,k}\right) \\ & + \frac{\mu_{p,k}}{2}\left\|\bar{\beta}_{p,k} - \beta_{p,k}\right\|_2^2, \end{aligned} \tag{12}$$

where $\bar{\beta}_{p,k} = \left[\frac{1}{L} \sum_{l=1}^{L} \mathbf{T}_l \boldsymbol{\beta}_l \right]_{p,k}$ is the averaging of local RCS estimations, for $p = 1, \cdots, P$ and $k = 1, \cdots, Q$. Here, $\mu_{p,k}$ is the augmented Lagrangian parameter.

1) Update of Local Imaging

In the m-th iteration, each automotive radar will update the local radar imaging $\beta_{l,p,k}^{(m+1)}$ for $l = 1, \cdots, L$ in parallel as

$$\beta_{l,p,k}^{(m+1)} = \arg\min_{\beta_{l,p,k}} f_{p,k} = \arg\min_{\beta_{l,p,k}} \left\{ \begin{array}{l} \frac{1}{2} \sum_{l=1}^{L} \|\mathbf{d}_l - \beta_{l,p,k} \mathbf{b}_{l,p,k}\|^2_{\mathbf{Q}_{l,p,k}^{-1}} \\ +\sigma_{p,k}^{(m)} \left(\bar{\beta}_{p,k}^{l} + \beta_{p,k}^{l} - \beta_{p,k}^{(m)} \right) \\ + \frac{\mu_{p,k}}{2} \left\| \bar{\beta}_{p,k}^{l} + \beta_{p,k}^{l} - \beta_{p,k}^{(m)} \right\|_2^2 \end{array} \right\}, \tag{13}$$

where $\bar{\beta}_{p,k}^{l} = \left[\frac{1}{L} \sum_{i \neq l}^{L} \mathbf{T}_i \boldsymbol{\beta}_i^{(m)} \right]_{p,k}$ and $\beta_{p,k}^{l} = \left[\frac{1}{L} \mathbf{T}_l \boldsymbol{\beta}_l \right]_{p,k}$. The objective function in (13) is differentiable with respect to $\beta_{l,p,k}$. Thus, $\beta_{l,p,k}^{(m+1)}$ can be obtained in closed-form by letting $\nabla_{\beta^*_{l,p,k}} f_{p,k} = 0$, which yields

$$\beta_{l,p,k}^{(m+1)} = \frac{\mathbf{b}_{l,p,k}^H \mathbf{Q}_{l,p,k}^{-1} \mathbf{d}_l - \frac{\left(\sigma_{p,k}^{(m)}\right)^* t_{l,p,k}}{L} - \frac{\mu_{p,k}}{L} \left(\bar{\beta}_{p,k}^{l} - \beta_{p,k}^{(m)} \right)}{\mathbf{b}_{l,p,k}^H \mathbf{Q}_{l,p,k}^{-1} \mathbf{b}_{l,p,k} + \frac{\mu_{p,k} t_{l,p,k}}{L^2}}, \tag{14}$$

where $t_{l,p,k} = \left[\mathrm{diag}\left(\mathbf{T}_l \right) \right]_{p,k}$ is the p, k elements of the diagonal entries of matrix $\mathbf{T}_l$.

2) Update of Global Imaging

The global imaging update is to minimize the following augmented Lagrangian

$$\beta_{p,k}^{(m+1)} = \arg\min_{\beta_{p,k}} \left\{ \begin{array}{l} \sigma_{p,k}^{(m)} \left(\bar{\beta}_{p,k}^{(m)} - \beta_{p,k} \right) \\ + \frac{\mu_{p,k}}{2} \left\| \bar{\beta}_{p,k}^{(m)} - \beta_{p,k} \right\|_2^2 \end{array} \right\}, \tag{15}$$

where $\bar{\beta}_{p,k}^{(m)} = \left[\frac{1}{L} \sum_{l=1}^{L} \mathbf{T}_l \boldsymbol{\beta}_l^{(m)} \right]_{p,k}$. The closed-form global imaging update is obtained as

$$\beta_{p,k}^{(m+1)} = \frac{\mu_{p,k} \bar{\beta}_{p,k}^{(m)} + \left(\sigma_{p,k}^{(m)} \right)^*}{\mu_{p,k}}. \tag{16}$$

Each automotive radar will need to share its information with all the other radars and the averaging of all local imaging results is carried out in a distributed fashion.

3) Update of Dual Variable

Withe the updated local and global imaging, the dual variable can be updated as

$$\sigma_{p,k}^{(m+1)} = \sigma_{p,k}^{(m)} + \mu_{p,k} \left(\bar{\beta}_{p,k}^{(m+1)} - \beta_{p,k}^{(m+1)} \right). \tag{17}$$

The collaborative radar imaging algorithm is summarized in Algorithm 1.

Algorithm 1 Collaborative Automotive Radar Imaging

Input: $\mathbf{d}_l$: measured radar raw data from the l-th radar; $\mathbf{T}_l$: transform matrices; $\{\mu_{p,k}\}$: weights; ϵ: precision level.

1: **initialization**: Initialize the local radar imaging estimation with delay and sum beamformer for each automotive radar $l = 1, \cdots, L$

$$\beta_{l,p,k}^{(1)} = \frac{\mathbf{b}_{l,p,k}^H \mathbf{d}_l}{\mathbf{b}_{l,p,k}^H \mathbf{b}_{l,p,k}}, \quad p = 1, \cdots, P, \quad k = 1, \cdots, Q$$

each radar initializes the global imaging using its local initial imaging $\boldsymbol{\beta}_G^{(1)} = \boldsymbol{\beta}_l^{(1)}$; initialize the dual variable $\boldsymbol{\sigma}^{(1)} = \mathbf{0}$; set $m = 1$

2: **while** $\left\| \boldsymbol{\beta}_G^{(m+1)} - \boldsymbol{\beta}_G^{(m)} \right\| \geq \epsilon$ **do**

3: In parallel, each radar update the local radar imaging $\boldsymbol{\beta}_l^{(m+1)}$ via equation (14), global radar imaging $\boldsymbol{\beta}_G^{(m+1)}$ via equation (16) and dual variables $\boldsymbol{\sigma}^{(m+1)}$ via equation (17).

4: Each radar shares its local and global radar imaging estimations $\boldsymbol{\beta}_l^{(m+1)}, \boldsymbol{\beta}_G^{(m+1)}$ and dual variables $\boldsymbol{\sigma}^{(m+1)}$ to radars on other automobiles.

5: $m = m + 1$

6: **end while**

Output : Global imaging $\boldsymbol{\beta}_G$

B. Coordinate Translation

Let $\mathbf{x}$ and $\mathbf{x}'$ denote the radar estimations under the local coordinate and global coordinate systems, respectively. The two coordinates are related via the following equation [18]

$$\mathbf{x}' = \mathbf{T}\mathbf{x} + \mathbf{t}, \tag{18}$$

where $\mathbf{T}$ is a two-dimensional rotation matrix with parameter of yaw θ, and $\mathbf{t}$ is a translational offset. Each radar needs to know the location of other neighboring radar is the networks. With the knowledge of other radars' locations, a transform matrix can be learned to compensate each radar's estimation result so that the estimations are aligned under the global coordinate system. An efficient method based on FFT has been proposed in [18] to estimate the rotation matrix. The calibration of target's position and oritentation was developed in [19]. A deep learning approach was proposed in [11] to estimate the translation matrix.

III. Numerical Results

We consider two automotive radars, one located at $(-20, 0)$ and the other one located at $(60, 0)$. Each radar has a uniform linear array with $N = 10$ elements and element spacing of half wavelength. For comparison, we compare the collaborative radar imaging with the standalone radar imaging approach using the iterative adaptive approach (IAA) algorithm [20].

Each automotive radar transmits FMCW chirps with bandwith of 300 MHz, chirp duration of 25.6 μs, pulse repetition interval of 30.4 μs. The sampling frequency is 10 MHz, and the number of samples in one chirp is 256. Each radar has a field of view (FOV) of $[-70°, 70°]$. Assume there

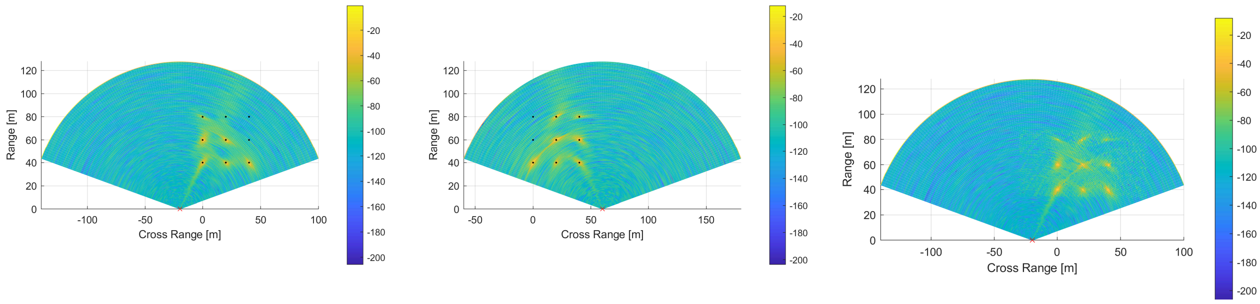

(a) (b) (c)

Fig. 2. The radar imaging of 9 targets, whose positions are denoted by •. (a) Local imaging of automotive radar at $(-20, 0)$ denoted by ×; (b) Local imaging of automotive radar at $(60, 0)$ denoted by ×; (c) Collaborative radar imaging achieved at $(-20, 0)$, which could also be achieved at $(60, 0)$.

are 9 point targets with coordinates of $x = 0, 20, 40$ and $y = 40, 60, 80$. The RCS of targets far away from the radar is set to zero. To construct the dictionary matrix $\mathbf{B}$, the range and FOV are discretized with range step of 0.5 m and angle step of $1°$.

The standalone radar imaging results obtained via IAA algorithm using local radar measurements are shown in Fig. 2 (a) and (b). It can be found that targets far away from each radar are not detected in standalone radar imaging. On the contrary, all the 9 targets are clearly and correctly detected via the collaborative radar imaging, as shown in Fig. 2 (c).

IV. Conclusions

In this paper, we developed a distributed collaborative automotive radar imaging approach to non-coherently fuse the radar imaging results from distributed automotive radar on adjacent vehicles. The collaborative radar imaging was shown to have significant improvement in perception performance by exploiting the spatial diversity.

Acknowledgement

This work was supported in part by U.S. National Science Foundation (NSF) under Grant CCF-2153386.

References

[1] S. Sun, A. P. Petropulu, and H. V. Poor, "MIMO radar for advanced driver-assistance systems and autonomous driving: Advantages and challenges," *IEEE Signal Processing Magazine*, vol. 37, no. 4, pp. 98–117, 2020.

[2] C. Waldschmidt, J. Hasch, and W. Menzel, "Automotive radar — From first efforts to future systems," *IEEE Journal of Microwaves*, vol. 1, no. 1, pp. 135–148, 2021.

[3] M. Markel, *Radar for Fully Autonomous Driving*. Boston, MA: Artech House, 2022.

[4] Z. Peng, C. Li, and F. Uysal, *Modern Radar for Automotive Applications*. London, UK: IET, 2022.

[5] S. Sun and Y. D. Zhang, "4D automotive radar sensing for autonomous vehicles: A sparsity-oriented approach," *IEEE Journal of Selected Topics in Signal Processing*, vol. 15, no. 4, pp. 879–891, 2021.

[6] A. Frischen, J. Hasch, and C. Waldschmidt, "A cooperative MIMO radar network using highly integrated FMCW radar sensors," *IEEE Trans. Microw. Theory Tech.*, vol. 65, no. 4, pp. 1355–1366, 2017.

[7] M. Gottinger and et. al., "Coherent automotive radar networks: The next generation of radar-based imaging and mapping," *IEEE Journal of Microwaves*, vol. 1, no. 1, pp. 149–163, 2021.

[8] M. Chowdhury and Y. D. Zhang, "Direction-of-arrival estimation exploiting distributed sparse arrays," in *Proc. 55th Annual Asilomar Conference on Signals, Systems, and Computers*, Pacific Grove, CA, Oct. 31 - Nov. 3, 2021.

[9] G. Zhang, T. Huang, Y. Liu, X. Wang, and Y. C. Eldar, "Direction finding in partly calibrated arrays exploiting the whole array aperture," *arXiv preprint arXiv:2212.04707*, 2022.

[10] S. L. Fernández, A. C. J. Samarasekera, R. Feger, and A. Stelzer, "Measurement-based analysis of a non-coherent MIMO radar network for automotive applications," in *European Radar Conference (EuRAD)*, Milan, Italy, Sept. 28-30, 2022, pp. 13–16.

[11] B. K. Chalise, D. M. Wong, M. G. Amin, A. F. Martone, and B. H. Kirk, "Detection, mode selection, and parameter estimation in distributed radar networks : Algorithms and implementation challenges," *IEEE Trans. Aerosp. Electron. Syst.*, to appear, 2022.

[12] S. Kong, S. Lee, C.-Y. Kim, and S. Hong, "Wireless cooperative synchronization of coherent UWB MIMO radar," *IEEE Trans. Microw. Theory Tech.*, vol. 62, no. 1, pp. 154–165, 2014.

[13] J. Nanzer, S. R. Mghabghab, S. M. Ellison, and A. Schlegel, "Distributed phased arrays: Challenges and recent advances," *IEEE Trans. Microw. Theory Tech.*, vol. 69, no. 11, pp. 4893–4907, 2021.

[14] R. Molina-Masegosa and J. Gozalvez, "LTE-V for sidelink 5G V2X vehicular communications: A new 5G technology for short-range vehicle-to-everything communications," *IEEE Veh. Technol. Mag.*, vol. 12, no. 4, pp. 30–39, 2017.

[15] L. G. de Oliveira, B. Nuss, M. B. Alabd, A. Diewald, M. Pauli, and T. Zwick, "Joint radar-communication systems: Modulation schemes and system design," *IEEE Trans. Microw. Theory Tech.*, vol. 70, no. 3, pp. 1521–1551, 2022.

[16] A. Murtada, R. Hu, B. Rao, and U. Schroeder, "Widely distributed radar imaging: unmediated ADMM based approach," *arXiv preprint arXiv:2203.05495*, 2022.

[17] S. Boyd, N. Parikh, and E. Chu, *Distributed Optimization and Statistical Learning via the Alternating Direction Method of Multipliers*. Now Publishers, 2011.

[18] R. Weston and at. al., "Fast-MbyM: Leveraging translational invariance of the Fourier transform for efficient and accurate radar odometry," in *IEEE Intl. Conf. on Robotics and Automation (ICRA)*, Philadelphia, PA, May 23-27, 2022, pp. 2186–2192.

[19] T. Grebner, M. Linder, N. Kern, P. Schoeder, and C. Waldschmidt, "6D self-calibration of the position and orientation of radar sensors in a radar network," in *European Radar Conference (EuRAD)*, Milan, Italy, Sept. 28-30, 2022, pp. 157–160.

[20] T. Yardibi, J. Li, P. Stoica, M. Xue, and A. Baggeroer, "Source localization and sensing: A nonparametric iterative adaptive approach based on weighted least squares," *IEEE Trans. Aerosp. Electron. Syst.*, vol. 46, no. 1, pp. 425–443, 2010.